

Chapter 1

The Phenomenon: Occurrence and Characteristics

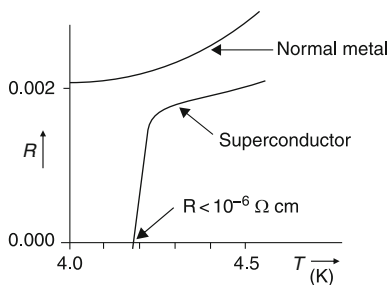
1.1 Marching Towards Absolute Zero

The phenomenon of superconductivity has been observed only at low temperatures. Therefore, we shall first consider the efforts made and the achievements on the way to absolute zero temperature.

A very common way of liquefying gases is to compress them. This causes the gas molecules to come closer, and the role of cohesive forces increases. This makes gas–liquid transition to become possible: However, at temperatures higher than the critical point, it is not possible to turn the gas into a liquid, however, large the pressure applied. So, it is necessary to cool the gas first before compressing it. In 1877, French scientist Cailletet succeeded in liquefying oxygen at a temperature 90.2 K. Six years later, N₂ was liquefied at 77.4 K. The hydrogen was found to be liquefied at a temperature of 20.4 K. This was made possible by sir James Dewar in 1898, who invented a vacuum vessel, which is used even nowadays to store liquid hydrogen. Helium was discovered in 1869 in the spectrum of solar corona. For a long time, it could not be detected on earth. It was only in 1895 that Sir William Ramsay found it among gases released when certain minerals were heated. At the end of nineteenth century, it became known that the boiling point of helium was even lower than that of hydrogen. In the late 1890s, Dutch scientist K. Onnes began his experiments aimed at liquefying helium. It was ultimately found that the transition temperature is 4.2 K and liquefaction was achieved in 1908.

Liquid helium is often called a quantum fluid. It is a striking demonstration of the fact that quantum behaviour may be manifested by macroscopic bodies as well. Liquid He remains a liquid even at absolute zero (even though at 0 °K, there would be no thermal motion at all). This is because of very low density of liquid helium; it is eight times lighter than water. Therefore, light and inert helium atoms are widely separated. Near absolute zero, the laws of quantum physics prevent it from becoming a solid, that is, the usual classical concept that: atoms are completely at rest at absolute zero is incorrect.

Fig. 1.1 Temperature dependence of resistance of a normal metal and a superconductor



Having attained recorded low temperatures and having obtained liquid helium, K. Onnes turned to undertake a systematic study of the properties of matter at low temperatures.

1.2 Discovery of Superconductivity

The attainment of liquid helium temperatures opened a new regime of low temperatures and it was discovered by K. Onnes in 1911, while investigating the electrical properties of frozen mercury when the electrical resistance of mercury completely disappeared on approaching 4.2 K. In his own words,

The experiment left no doubt that as far as the accuracy of measurement went, the resistance disappeared. At the same time, however, some thing unexpected occurred. The disappearance did not take place gradually, but abruptly. From 1/500, the resistance at 4.2 K drops to a millionth part. At the lowest temperature, 1.5 K, it could be established that the resistance had become less than a thousand-millionth part of that at normal temperature. Thus, the mercury at 4.2 K has entered a new state, which, owing to its particular electrical properties, can be called the state of superconductivity.

The phenomenon of superconductivity is manifested in the electrical resistance vanishing at a finite temperature called the critical temperature and denoted T_c (Fig. 1.1). The latest data show that the resistivity of a superconductor is below $10^{-27} \Omega\text{-cm}$. This can be compared with the resistivity of copper (an excellent conductor), which is $10^{-9} \Omega\text{-cm}$. So, there is no doubt that we are dealing with ideal conductivity (total vanishing of electrical resistance).

K. Onnes discovery was followed by a large number of experimental studies. New superconducting materials were further discovered and their physical properties were studied.

1.3 Occurrence of Superconductivity

Superconductivity has been found to be exhibited by many elements: alloys, binary and ternary compounds, organic superconductors and lately discovered (1986) high T_c superconductors.

1.3.1 Elemental Superconductivity

Superconductivity in elements is displayed by non-transition metals, e.g. Be ($T_c = 0.03$ K), Al (1.19 K), Pb (7.0 K), Sn (3 K). Examples of superconducting transition metals are Nb (9.2 K), Mo (0.92 K), Zn (0.9 K). Semiconductor elements, which display superconductivity are Si (8.3 K at 165 kbar pressure), Ge, Se and Te. Semimetal Bismuth also shows superconductivity depending on its crystal structure (Different modifications show different transition temperatures and one modification does not show superconductivity down to 10^{-2} K). Ferromagnetic materials (Fe, Co, Ni) do not display superconductivity.

1.3.2 Alloys

A large number of alloys display superconductivity with a relatively high transition temperature, e.g. Nb–Ti is important in cryogenic applications and $\text{Nb}_3\text{Al}_{0.75}\text{Ge}_{0.25}$ has a T_c of 20.7 K.

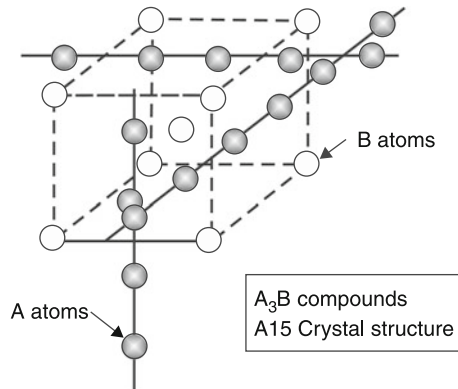
1.3.3 Binary Compounds (A-15 Materials)

Some binary compounds also show superconductivity. These are the so called A-15 compounds discovered by G.E. Hardy and J. Hulme in 1954.

Until the discovery of the high T_c superconductors (i.e. prior to 1986), most of the highest T_c superconducting materials all had the crystal structure illustrated in Fig. 1.2. The stoichiometry (the relative composition of constituent atoms mandated by the ideal crystal structure) of the material of this class is A_3B , where A is one of the transition metals (such as Nb, V, Ta or Zr) and the B atom comes from the IIIA or IVA column of the periodic table and is a metal or semiconductor, such as Sn, Al, Ga, Ge, In or Si.

The A elements are situated at the corners of a cube and the B elements form three orthogonal chains the T_c s of a few A-15 compounds are

Fig. 1.2 Structure of A15 materials



$V_3Ga(16.5K)$, $Nb_3Ge(23.2K)$,
 $V_3Si(17K)$, $Nb_3Al(17.5K)$,
 $Nb_3Sn(18K)$.

The niobium compounds have typically the highest transition temperature with that of Nb_3Ge (23.2 K) being the highest one. The T_c is quite sensitive to the stoichiometry and the maximum T_c corresponds to the ratio being just 3:1 of the ordered material.

1.3.4 Heavy Fermion Superconductors

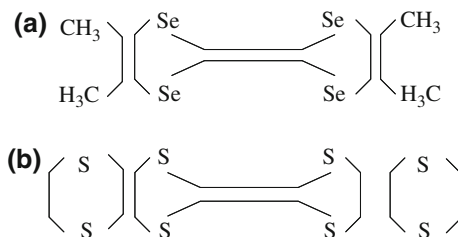
These are contemporary of organic superconductors and were discovered in 1979 by Steglich et al. [1]. These are characterised by low value of T_c , for example: $CeCu_2Si$ (0.5 K), UBe_{13} (0.85 K) and UPt_3 (0.5 K). Their names reflect their important feature: the effective mass is several hundred times greater than that of a free electron. The superconducting state displays some anomalous properties. In conventional superconductors, the electronic heat capacity decreases exponentially with temperature, whereas in heavy fermions superconductors, a power law decrease is observed.

1.3.5 Organic Superconductors

These are an unusual class of superconductors, which are insulators in normal state (with very low conductivity).

The first organic superconductor was discovered by Jerome et al. in 1980 [2] with T_c of only 1 K. However, in 1990, an organic superconductor with a T_c of 12 K was synthesised. At present, there are two known classes of organic superconductors. One of them is described by the chemical formula $(TMTSF)_2X$. The TMTSF (*Tetra*

Fig. 1.3 **a** The TMTSF molecule **b** The BEDT-TTF molecule



methyltetra selenaful valene) structure is shown in Fig. 1.3a, where X is a monovalent inorganic anion. Typical anions are PF_6^- , AsF_6^- and NbF_6^- .

The other class is formed by materials with the composition $(\text{BEDT-TTF})_2\text{X}$. The *bis-ethylene dithio tetra thia ful valene* (BEDT-TTF) molecule is shown in Fig. 1.3b, where X is again a monovalent anion.

The crystal $(\text{BEDT-TTF})_2\text{I}_3$ has $T_c = 8.1$ K.

1.3.5.1 High Temperature Superconductors

These oxide superconductors are defect perovskite like cuprate materials, which were discovered lately in 1986 by Bednorz and Müller (They were awarded the Nobel prize for their remarkable discovery) [3]. This discovery waited for nearly 70 years after the discovery of superconductivity. These materials have T_c s as high as 90–125 K (prior to this, T_c achieved was below 23.2 K, corresponding to that of Nb_3Ge). Bednorz and Muller discovered high temperature superconductivity ($T_c \sim 35$ K) in defect perovskite like oxide material $\text{La}_{2-x}\text{Ba}_x\text{CuO}_4$. These materials are layered structures in which sheets of copper and oxygen atoms alternate with sheets of rare-earth (and oxygen) atoms. Soon after, Paul Chu and his coworkers [4] discovered the so called 123 oxides of the general formula $\text{LnBa}_2\text{Cu}_3\text{O}_{7-\delta}$ ($\text{Ln} = \text{Y}, \text{Nd}, \text{Sm}, \text{Eu}, \text{Gd}, \text{Dy}, \text{Ho}, \text{Er}, \text{Tm}$ or Yb) with T_c values in the 90 K region. The discovery of materials with superconductivity above the liquid- N_2 temperature raised much hope and prompted intensive search for new classes of oxides with still higher T_c s. Two series of compounds belonging to the Bi–Sr–Ca–Cu–O and Tl–Ba–Ca–Cu–O systems have been found to exhibit superconductivity between 60 and 125 K [5, 6].

It is noteworthy that all the high T_c cuprates possess “defect perovskite layers” and all except 123 compounds contain rock salt type oxide layers. The crystal structure of perovskite and rock salt type layers are shown in Fig. 1.4.

The structure in bulk corresponds to K_2NiF_4 structure, depicted in Fig. 1.5 (La_2CuO_4). In this Ba/Sr is substituted on Lanthanum sites. The perovskite layers consist of corner sharing CuO_6 octahedra.

Some important superconductors, their T_c s and year of discovery are given in Table 1.1.

In the La based, Y-based, Bi-based, Tl-based and Hg-based cuprate families, the carriers of superconducting current are electron-vacancies or holes (pairs).

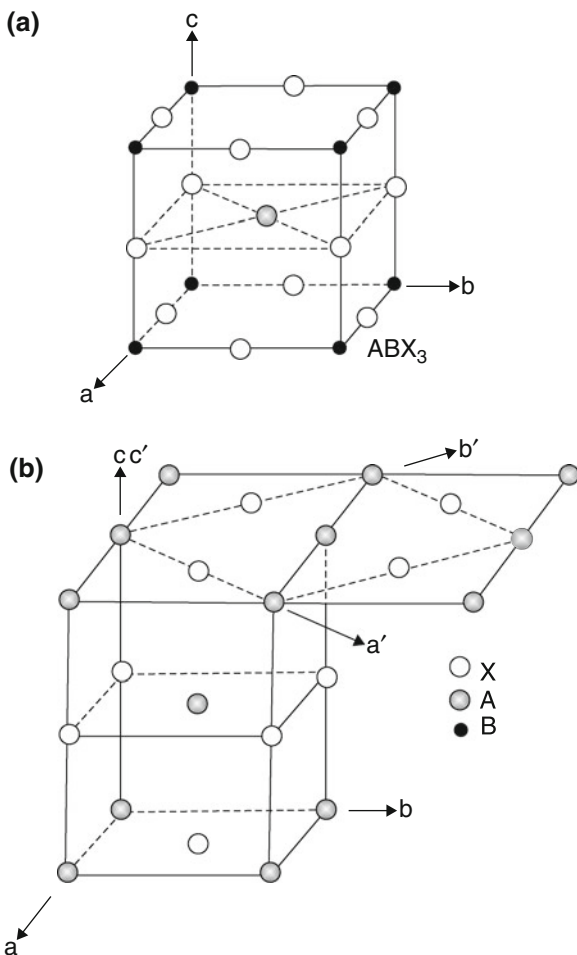


Fig. 1.4 Crystal structure of **a** perovskite and **b** rock salt. The conventional unit cell is face centered and is defined by axes a' , b' and c'

By contrast, in the HTSC discovered in 1989 ($\text{Nd}_{2-x}\text{Ce}_x\text{CuO}_4$), the carriers are electron-pairs as verified by Hall-coefficient measurement.

1.3.6 C_{60} -Based Superconductors

The C_{60} molecule (termed as *Buckminster fullerene*) consisting of a geodesic sphere of 60 carbon atoms was discovered by Richard Smalley (USA) and Harry Kroto (England) and their discovery appeared in “Nature” (14 Nov. 1985). By doping C_{60}

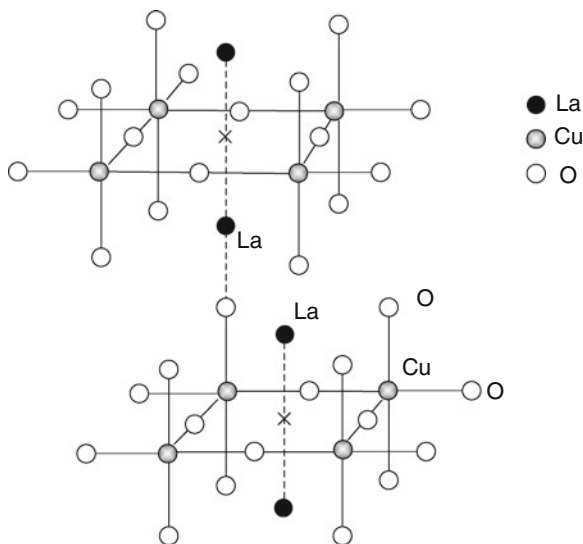


Fig. 1.5 K_2NiF_4 structure (La_2CuO_4)

with potassium atoms, Hebard et al. [7] obtained superconductivity at 18 K in K_xC_{60} . Rb-doped C_{60} produced superconductor with a $T_c \sim 28$ K. In 1991, S.P. Kelty et al. reported superconductivity at ~ 30 K in Cs doped C_{60} , however, the superconducting phase was less stable than K- and Rb-doped superconductors.

Figure 1.6 shows various superconductors discovered, their T_c s versus year of discovery. It is to be conjectured here that attainment of liquefaction of gases like O_2 (at 90.2 K), N_2 (at 77.4 K), H_2 (at 20.4 K) and then He (at 4.2 K) were important milestones in the area of cryogenics (low temperature physics). The discovery of high T_c materials with superconductivity well above boiling point of liquid nitrogen (LN_2) was, therefore, a notable discovery from the viewpoint of technological applications. Further, availability of these materials raised the hopes for reducing the cost of cryogenics involved in operating at LN_2 temperatures compared to that operating at liquid-He temperatures. (LN_2 costs only 20 Rupees per litre, whereas liquid-He costs about 1,000 times higher). As a consequence, thermal insulation required for cryostats was also reduced.

1.4 The Superconducting State

The fact that apparently there is no scattering of electrons by the atoms of the crystal lattice leads to the conclusion that the wave function describing the electrons in the superconducting state must be different substantially from those in the normal state. Since (in superconducting state) lattice periodicity has no influence on the

Table 1.1 Some important superconductors

Material	Highest T_c (K)	Year of discovery	Discovered by
Hg	4.1	1911	K. Onnes
Pb	7.2	1913	—
Nb	9.2	1930	—
Nb ₃ Sn	18.1	1954	—
NbTi	9.5	1961	—
TiO, NbO	1	1964	—
SrTiO _{3-x}	0.7	1964	—
A ₃ WO ₃	6	1965	—
A ₃ MoO ₃	4	1969	—
A ₃ ReO ₃	4	1969	—
V ₃ Ga	14.5	1966	—
PbMo ₅ S ₆	15.0	1972	—
Nb ₃ Ge	23.3	1973	J. R. Gevaler
Ba(Pb, Bi)O ₃	13	1975	—
(La, Ba) ₂ CuO ₄	35	1986	J. G. Bednorz and K. A. Muller
YBa ₂ Cu ₃ O ₇	90	1987	M. K. Wu and C. W. Chu
Bi–Sr–Cu–O	22	1987	Michel et al.
Bi–Sr–Ca–Cu–O	100	1987	Maeda and Tarascan
Tb–Ba–Ca–Cu–O	122	1988	Sheng and Hermann
Hg–Ba–Ca–Cu–O	130	1992	Putilin and A. Schilling
Ln _{2-x} Ce _x CuO _{4+y} (Lx = Pr, Nd, Sm)	25	1989	Tokura, Takagi and Uchida

electrons, therefore, the wave function is not localised but has infinite extent. In view of the uncertainty relation, this implies a precisely definite momentum. Ground state (superconducting state) is described by

$$\psi_G = \psi(r_1, r_2) \psi(r_3, r_4) \dots \psi(r_{n_s-1}, r_{n_s})$$

where n_s = number of super electrons (there are $n_s/2$ pairs), i.e. the wave function is product of the pair wave functions. All the pairs have the same wave function given by

$$\psi(r', r'') = \sqrt{n_s} e^{iS(\vec{r})},$$

where the phase function $S(\vec{r})$ characterises the coherent state.

As the temperature is lowered, the electrons having energy close to Fermi energy get a chance to interact with ion-lattice via phonons due to reduced scattering at low temperatures. As a result, Cooper pairs get formed, the length scales over which their motion is correlated is the *coherence-length*:

$$\xi(T) = \frac{0.74 \xi_0}{\sqrt{(1-T)}}; \quad \xi_0 = \frac{\hbar v_F}{\pi \Delta_0},$$

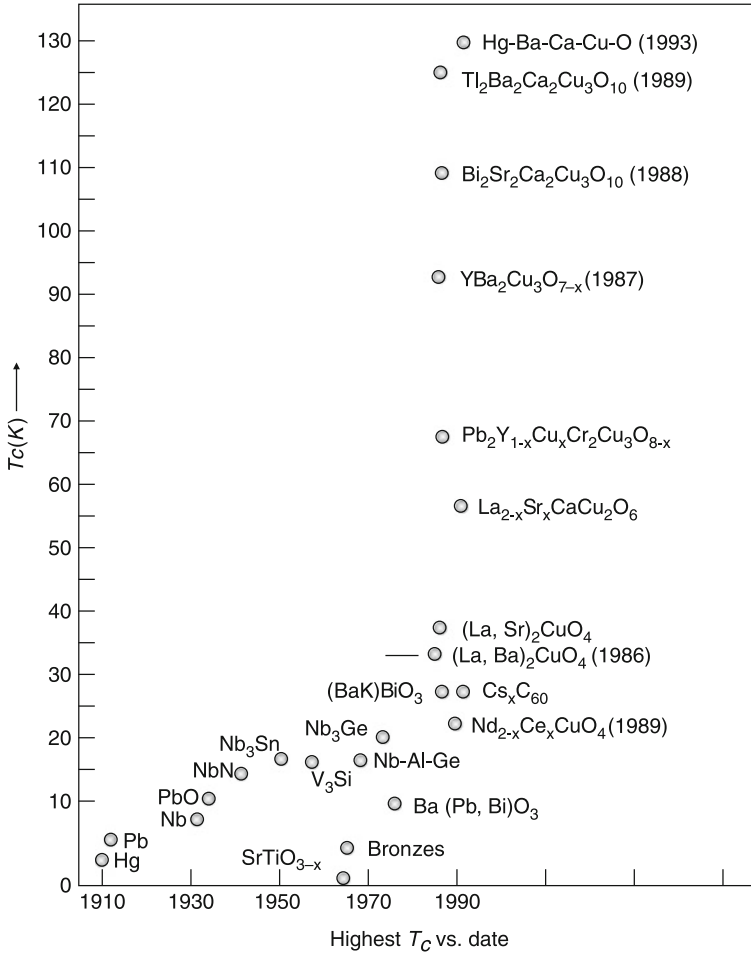


Fig. 1.6 Critical temperature versus year of discovery

where, v_F is the fermi velocity and Δ_0 is the energy gap (at 0°K), which is the gap between superconducting pairs and normal electrons. *The paired electrons move without resistance, whereas single electrons do not:*

Before pairing, electrons are separate entities (Fermions) having random momenta (due to scattering). When pairs form, two electrons of a pair have zero net momentum and opposite spins, so that in current carrying state they do not under go incoherent scattering, i.e. a pair is like a singlet and all pairs acquire same momentum in the same direction. Same momenta implies the same value of phase gradient for all pairs (momentum $\vec{P} = \hbar \nabla S = 2mev$). Therefore, there will be no change in current flow. Their motions are correlated (*Phase coherence*). The only scattering event, which

will reduce the current will be when a pair is imparted with an energy greater than the binding energy of the pair (i.e. $\geq \Delta_0$).

For $I < I_c$, there is no way to impart this energy. The long range coulomb repulsion between two electrons of a pair has been largely suppressed by screening due to strong correlation effects of the other electrons.

1.5 Phase Coherence

The superconducting ground state is represented by many electron wave function

$$\psi_G(\vec{r}_1, \vec{r}_2, \dots, \vec{r}_{n_s}) = \phi(\vec{r}_1, \vec{r}_2) \phi(\vec{r}_3, \vec{r}_4) \cdots \phi(\vec{r}_{n_s-1}, \vec{r}_{n_s}),$$

where total number of pairs equals $n_s/2$. \vec{r}_n is the position coordinate of n th electron and the ϕ 's are the same for all pairs. The local super fluid density is given by

$$n_s(\vec{r}) = |\psi_G(\vec{r})|^2 \quad (1.1)$$

and the super-current density is expressed by

$$\vec{J}(\vec{r}) = -i \frac{e\hbar}{2m_e} [\psi_G^* \nabla \psi_G - \psi_G \nabla \psi_G^*] - \frac{e^2}{m_e} \vec{A}(\vec{r}) \psi_G^* \nabla \psi_G \quad (1.2)$$

$\vec{A}(\vec{r})$ is the vector potential ($\vec{B} = \nabla \times \vec{A}$).

For steady state conditions, ψ_G or ψ can be written

$$\begin{aligned} \psi(\vec{r}) &= \psi_0 e^{iS(\vec{r})} \\ &= (n_s)^{1/2} e^{iS(\vec{r})} \end{aligned} \quad (1.3)$$

where the phase $S(\vec{r})$ is a real function of position \vec{r} . Then, (1.2) becomes

$$\begin{aligned} \vec{J}_s &= \frac{n_s}{2} \frac{e}{m_e} (\hbar \nabla S - 2e \vec{A}) \\ (\because \psi^* \psi &= 1) \end{aligned} \quad (1.4)$$

(assuming that condensate in superconductor can be represented by a macroscopic wave function in the form of (1.3)).

We anticipate that the condensate is made up of pairs of electrons of number density $n_s/2$, mass $2m_e$ (and charge $2e$).

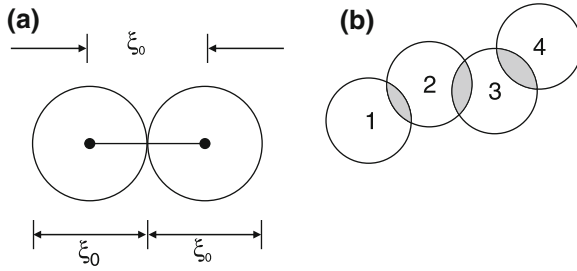


Fig. 1.7 **a** The pairs centre of mass phases are locked over a distance ξ **b** establishment of long range phase order

Equations (1.3) and (1.4) imply we cannot describe a super-current in a homogeneous material, unless $\psi(\vec{r})$ is complex. The physical situation depends on the variation of the phase and not simply on the magnitude of ψ .

From (1.4),

$$m^* \vec{v}_s(\vec{r}) = \hbar \nabla S(\vec{r}) - e^* \vec{A}(\vec{r}). \quad (1.5)$$

In the absence of a magnetic field, the phase function $S(\vec{r})$ plays the part of a velocity potential for the super fluid velocity \vec{v}_s . Therefore, if S did not vary in space, there would be no super-current. The phase function $S(\vec{r})$ characterises the electron ordering, represents the same phase of all pairs (phase coherence).

In the absence of \vec{A} , the local value of S varies with position at a rate proportional to v_s , i.e. $\nabla S \propto \vec{v}_s$ along the direction of flow.

1.6 Coherence Length

The maximum distance between electrons of a cooper-pair in real space upto which their motion is correlated (by taking advantage of the attractive interaction) is known as the *Coherence length* (ξ_0).

The pairs control the local phase order within a superconductor. All pairs lying in a sphere of diameter ξ_0 have the same centre-of-mass-momentum and the same centre-of-mass-phases.

In Fig. 1.7b, circles represent spheres of diameters ξ . Starting from sphere 1, we note that in the region of overlap with sphere 2, the phases must be same. Thus, if sphere 2 locks phases within it, phase-locking is continued from the basic length to the entire superconductor (by overlapping spheres of diameter ξ_0), establishing a long range phase order (Coherence).

The phase continuation (i.e. coherence) is forced by virtue of condensation energy associated with the overlap regions between two spheres.

1.6.1 Pippard's Equation and Coherence Length

If one looks at the expression of penetration depth as given by

$$\lambda = \sqrt{\frac{m}{\mu_0 n_s e^2}} \quad (\text{see article 1.14})$$

then impurities in a material should not change appreciably the penetration depth. Pippard did an experiment by measuring the microwave surface impedance of Sn diluted with small amounts of indium at about 3 cm wavelength and estimated the penetration depths from the surface impedance values. According to London's theory, there should not be an appreciable change in the penetration depth of Sn, but Pippard observed that penetration depth changes roughly by a factor of 2 at low temperatures, and this led to the non-local modification of the London theory and the concept of (electromagnetic) coherence length ξ , which depends on the mean free path.

We have,

$$\vec{H} = -\frac{m}{\mu_0 n_s e^2} \text{curl } \vec{j}_s. \quad (1.6)$$

$$\text{Therefore } \vec{A} = -\frac{m}{\mu_0 n_s e^2} \vec{j}_s \quad (\because \vec{H} = \nabla \times \vec{A}) \quad (1.7)$$

Pippard postulated that current density at any point in the superconductor depends on the vector potential \vec{A} not at that point, but integrated over a domain of radius ξ known as (Pippard's) coherence length. ξ must depend on the mean free path of the electrons to account for the variation of penetration depth with impurity content. The current-density is given by the generalised expression (Fig. 1.8)

$$\vec{j}_s(\vec{r}) = \int K(\vec{r}, \vec{r}') \vec{A}(\vec{r}') d\vec{r}' \quad (1.8)$$

The width of the Kernel function $K(\vec{r} - \vec{r}')$ defines the Pippard's coherence length (ξ). Pippard suggested the form of the kernel as

$$K(\vec{r}, \vec{r}') = \exp \left[-\frac{(\vec{r} - \vec{r}')}{\xi} \right] \quad (1.9)$$

$$\text{with } \frac{1}{\xi} = \frac{1}{\xi_0} + \frac{1}{\alpha \Lambda}. \quad (1.10)$$

Here, ξ is electromagnetic coherence length, which is of the order of 10^{-4} cm, α is an empirical constant (of the order of unity) and Λ is mean free path (ξ_0 is known as intrinsic coherence length).

The appearance of the electron mean free path shows that the coherence length is reduced by the presence of impurities and the ratio

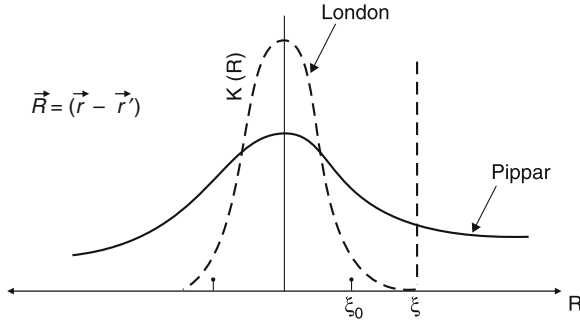


Fig. 1.8 Kernel function $K(R)$ versus R (representation of Coherence length)

$$k = \frac{\lambda}{\xi} \quad (\text{where } l \text{ is penetration depth})$$

is a number known as *Ginzberg Landau parameter*. It is controlled by alloying or doping a superconductor.

1.6.2 The Size of an Electron Pair

The spatial spread of electrons in a Cooper pair is, (using uncertainty relation)

$$\delta r = \frac{\hbar v_F}{\Delta}$$

where v_F is Fermi velocity.

The coherence length (size of the Cooper pair) is described by

$$\xi_0 = \frac{\delta r}{\pi} \equiv \frac{\hbar v_F}{\pi \Delta}. \quad (1.11)$$

It characterises the scale of spatial correlation in a superconductor. Substituting for v_F and Δ , we find

$$\xi_0 \cong 10^{-4} \text{ cm.}$$

Period of a crystal lattice is $\sim 10^{-8}$ cm. Thus, $\xi_0 \cong 10^4 \times$ lattice spacing. This indicates a long range correlation in a superconductor, which is unique in the inorganic world.

1.6.3 Analogy Between Long Range Spatial Order in a Solid and Phase-Order in a Superconductor

In a solid, the typical range of inter-atomic forces are \sim inter-atomic spacing. Once a part of the crystal forms the continued propagation, the order is established in a step-wise manner with the arrangement of the occupied sites legislating the arrangement of subsequent level through the short range interactions (\sim inter-atomic spacing).

In case of a superconductor, we are dealing with an interaction whose “range” is associated with the retarded nature of the phonon-exchange interaction.

Since the important lattice frequencies are of the order of the Debye frequency (ω_D), an electron with velocity (v_F) can come from a distance (v_F/ω_D) to feel the lattice disturbance produced by another electron. Thus, in a superconductor, the phonon exchange interaction may “extend” on the order of $\frac{v_F}{\omega_D} \approx 10^{-5}$ cm. The attractive nature of interaction leads to the formation of pairs, which are spread out over a coherence length ξ (which is $\sim 10^{-4}$ cm). The center of mass coordinates of some 10^6 pairs lie in a sphere of diameter ξ . For the attractive electron–phonon attraction to be taken advantage of, by each of the pairs, the space–time correlation are to be such that all have the same center-of-mass momentum. More generally, in presence of electromagnetic fields, we may extend this to the statement that the pairs must have the same center-of-mass phase. To the extent that they do not, the condensation energy is lost (This is how a short range force produces a long range order).

Therefore, just as atoms of a solid control the local spatial order around them, pairs (in a superconductor) control the local phase-order (within a coherence length).

1.7 Critical Magnetic Field

It was discovered by K. Onnes that application of magnetic fields destroy superconductivity. The minimum magnetic field necessary to vanish superconductivity is called the critical magnetic field. It is found to be dependent on temperature and is given by

$$H_c(T) = H_c(0) \left[1 - \left(\frac{T}{T_c} \right)^2 \right]. \quad (1.12)$$

This is known as *Tuyn’s law* $H_c(0)$ is the critical field at absolute zero. $H_c(0)$ and T_c are constants and characteristic of the material (Fig. 1.9).

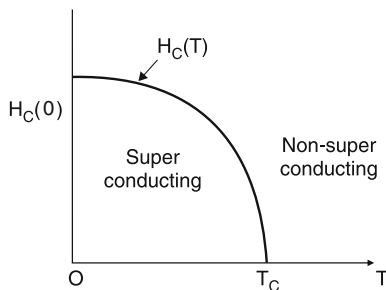


Fig. 1.9 Critical magnetic field as function of temperature

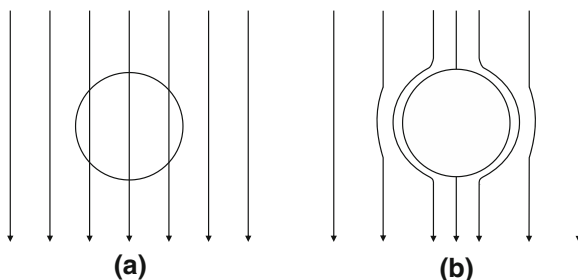


Fig. 1.10 The Meissner effect **a** For $T > T_c$ or $H > H_c$, normal conductor **b** $T < T_c$ and $H < H_c$, material is superconductor

1.8 Meissner Effect

In metals, other than ferromagnetic, the magnetic fields created by the elementary atomic currents are oriented chaotically in the metal and cancel out, therefore, magnetic induction $B = 0$ in the absence of an external field. In presence of an external field H , there appears a finite induction $\vec{B} = \mu \vec{H}$, where μ is the permeability

$\mu > 1$ (for paramagnetics),

$\mu < 1$ (for diamagnetics),

$\mu = 0$ (for superconductors),

i.e. in the superconducting state, a superconductor exhibits perfect diamagnetism. Meissner effect is the phenomenon, which relates diamagnetism with superconductors. This as follows:

Meissner and Ochsenfeld discovered in 1933 that below the critical temperature ($T < T_c$), if a superconductor is placed in a magnetic field, the magnetic field is expelled from the interior of a superconductor. This is known as *Meissner effect* (Fig. 1.10). Further, if $H > H_c$ (or $T > T_c$), the flux penetrates the superconductor, because then the material is non-superconducting and behaves like a normal conductor.

The point noteworthy here is that not only a magnetic field is excluded (for $T < T_c$) as the superconductor is placed in a magnetic field, but also a field present in an originally normal sample is expelled. This reversible nature of the Meissner effect is related thermodynamically to the free-energy difference between the normal and superconducting states in zero field, the so called *condensation energy* of the superconducting state, i.e.

$$f_n(T) - f_s(T) = \frac{H_c^2(T)}{8\pi} \quad (\text{c.g.s.unit}), \quad (1.13)$$

where f_n and f_s are the Helmholtz free energies/volume in the respective phases in zero field.

1.9 Comparison Between a Superconductor and a Very Good (or Ideal) Conductor

The electron–lattice interaction is the basic mechanism of electrical resistance in an ordinary metal. Metals, such as Au, Ag and Cu are excellent conductors but do not display superconductivity, because very good conductivity indicates that electrical resistance is very low. Therefore, the interaction between electrons and lattice is very weak, which at low temperatures does not create sufficient inter-electron attraction to overcome the coulomb repulsion. Therefore, there is no transition to superconducting state.

A perfect conductor does not exhibit Meissner effect, i.e. no flux expulsion on cooling:

In fact, the magnetic behaviour of an ideal conductor depends on whether the sample is first cooled to below T_c before applying the field (1) or the field is applied and then cooled (2).

For a superconductor, the final states are identical, regardless of whether B_{ext} is switched on before, or after cooling.

For any closed path enclosing an area “ a ” in a material, it must be true that

$$IR = V = \iint \text{curl } \vec{E} \cdot d\vec{a} = -\frac{\partial \vec{B}}{\partial T} \cdot \vec{A} \quad (1.14)$$

(using Maxwell’s equation) vanishing resistance implies magnetic flux $\vec{B} \cdot \vec{A}$ through the loop may not alter, that is, magnetic field inside must be maintained (what was initially there) both after cooling and after switching off the external field B_{ext} .

On switching off B_{ext} in the cooled state, this requirement is satisfied (in both A and B, Fig. 1.11), because the process of switching off B_{ext} induces persistent currents inside the material surface, which maintain the value of magnetic field in the interior. Now, in sense of (1.14), an ideal conductor (for $B_{\text{ext}} = 0$ and $T < T_c$) may adopt

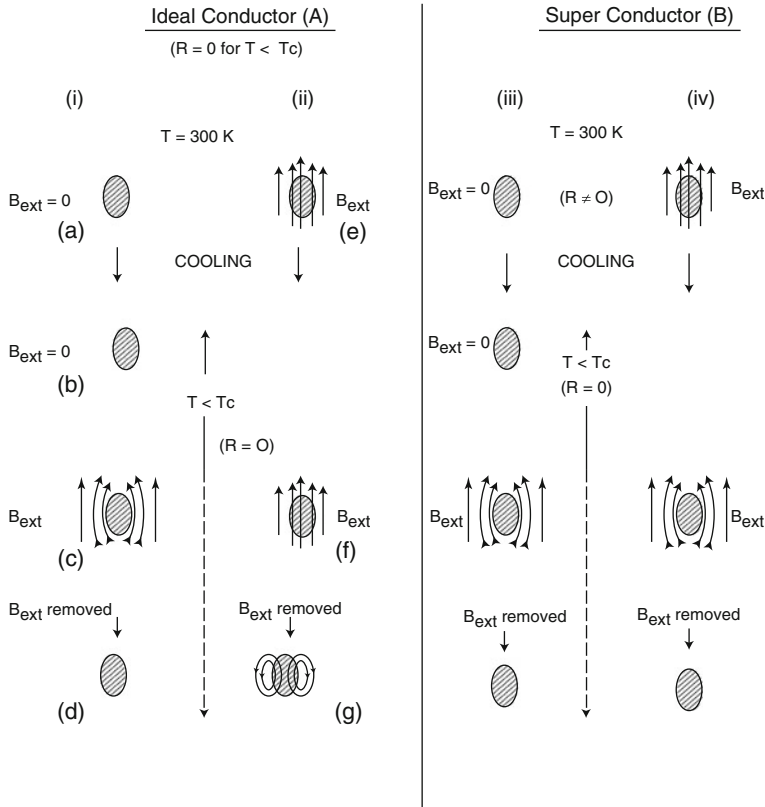


Fig. 1.11 Comparison of magnetic behaviours of an ideal conductor and a superconductor. Both have $R = 0$ for $T < T_c$

two different states ((c) or (f)) depending on the order of events leading to this state. Thus, we have two different states (d) and (g) for an ideal conductor. However, if a superconductor was merely such an “ideal conductor”, the superconducting state would not be a state in the thermodynamic sense. In fact, in the superconductor, not only $\frac{\partial \vec{B}}{\partial T} = 0$, but also $\vec{B} = 0$ independent of the path by which the state (c) or (f) is reached.

This Meissner effect, which represents the property of ideal diamagnetism (for a superconductor) follows independent of vanishing of electrical resistance. However, an ideal conductor does not show ideal diamagnetism (as evident from state (g)), i.e. external field is not expelled, if cooling is done after the application of external field.

Table 1.2 Values of isotope effect coefficient for some elements

Element	β
Sn	0.46
Mg	0.5
Ru	0(± 0.05)
Zr	0(± 0.05)
Mo	0.33
Os	0.21

1.10 Isotope Effect

Historically, the isotope effect has been instrumental in understanding the mechanism responsible for Cooper-pair formation in conventional superconductors. It has been observed experimentally that the superconducting transition temperature T_c varies with the isotopic mass M of the material as

$$T_c \propto M^{-\beta} \quad (1.15)$$

$$\text{Or } -\frac{d(\ln T_c)}{d(\ln M)} \equiv \beta \quad (1.16)$$

where β is called the isotope effect coefficient and is given by (BCS theory) as

$$\beta = 0.5[1 - 0.01\{N(0)V\}^{-2}] \quad (1.17)$$

where $N(0)$ is the density of single particle states for one spin at the Fermi level and V is the potential between the electrons. β has the value 0.4–0.5 for many superconductors, however, there are some notable exceptions (see Table 1.2).

Isotope effect was first discovered in mercury. It has been found that in mercury T_c varies from 4.185 K to 4.146 K, as isotopic mass varies from 1.995 amu to 203.4 amu. Since, Debye temperature θ_D is proportional to the velocity of sound, which varies as $M^{-1/2}$, therefore, T_c can be related to θ_D as

$$T_c \propto \theta_D \quad \text{or} \quad T_c/\theta_D = \text{a constant.} \quad (1.18)$$

Since Debye temperature depends on lattice vibrations, the above relation implies that lattice vibrations play an important role in superconductivity, as also suggested by Frohlich prior to the BCS theory.

The departure in values of β from 0.5 could be explained by Eliasberg theory, taking into consideration the competition between (1) electron-phonon interaction and (2) the Coulomb-repulsion.

1.11 Isotope Effect in HTSCs

Many experimental data indicate that the new high T_c oxides display many features of the BCS theory, such as carrier pairing and the presence of an energy gap. The pairing is caused by some intermediate field (may be other excitations like plasmons, excitons or magnons).

It still remains to figure out, which of these excitations are responsible for inter-electron attraction. Higher T_c s of cuprates does not imply presence of non-phonon mechanisms. The interest in investigating pairing mechanism in the cuprates has included much discussion on the relevance of the electron–phonon coupling mechanism (which is responsible for superconductivity in conventional superconductors). There have been several experimental indications of the isotope shift of T_c , due to presumably strong electron–phonon interactions. The indications are in the vibrational behaviour: Experiments performed on high T_c oxides with oxygen isotopic substitution yielded a very small shift of T_c . Similar results were obtained by Cu and Ba isotopic substitution.

1.11.1 Optical Behaviour Study

1. In 1987, it was identified infra-red active modes in LSCO (i.e. La–Sr–Cu–O) at 240 and 495 cm^{-1} . These arise from coupling of optic phonons to the electronic system.
2. It has been inferred from a number of studies that observation of Raman active and infra-red active modes with strong temperature dependent frequencies and line widths are due to electron–phonon coupling (Anharmonicity may be another possibility).
3. In 1988, Zeyner and Zwicky provided a theoretical analysis of the temperature dependence of Raman- and infra-red active modes in YBCO system, which indicates that this material is in the strong electron-phonon coupling limit.

1.11.2 Elastic and Ultrasonic Studies

These show, however, anomalies in their temperature dependence often closely correlated with T_c , which reflect strong electron–phonon coupling.

The character and strength of the electron–phonon interaction are of central interest, both for understanding the unusual physical properties of the cuprates as well as for describing the electronic system itself.

The electron–phonon interaction has been discussed widely as a possible pairing mechanism and, also as an impossible pairing mechanism for producing $T_c \sim 100\text{ K}$.

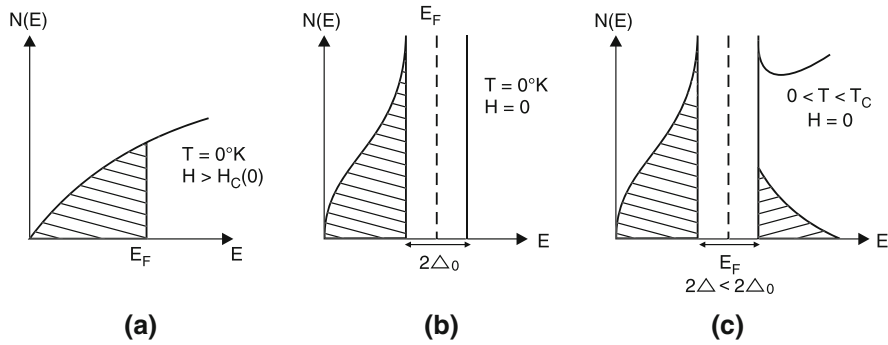


Fig. 1.12 Density and occupancy of states: **a** in absence of superconductivity, **b** in superconducting ground state, **c** superconducting state at finite temperature

The isotope-shift of T_c initially expected to be the crucial experiment, has not been as conclusive as was naively expected at first.

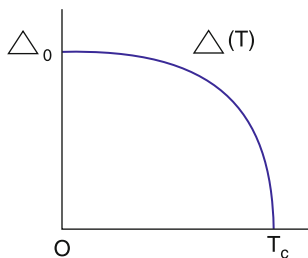
The smaller and negative values of the β could be explained with the help of Eliashberg theory, only if $T_c \sim 1$ K or less. In case of early results on cuprates, the oxygen isotope effect (with $T_c \sim 100$ K) showed $\beta_{\text{ox}} \sim 0$ (implying a result inconsistent with the electron phonon model), and therefore, the electron–phonon model was abandoned, favouring an electronic model. Many electronic models have been proposed but none yet completely expected. However, a smaller value of β_{ox} can be accounted for by considering (at the cost of some accuracy) a joint phonon, but largely electronic mechanism.

Recently “strange isotope-effect” has been observed, which has added to the confusion, a rapid variation in the β_{ox} value is found (even > 0.5) with doping variation (so as to change T_c), e.g. rapid increase in β for $\text{Y}_{1-x}\text{Pr}_x\text{Ba}_2\text{Cu}_3\text{O}_7$.

1.12 The Energy Gap

The behaviour of the specific heat in the superconducting state is a strong indication of the existence of an energy gap in the excitation spectrum of the electrons in the conduction band. Figure 1.12b illustrates this by comparing the difference between the occupancy of states in a normal metal (Fig. 1.12a) and a superconductor. Figure 1.12b illustrates the superconducting ground state for absolute zero temperature. This shows a zero density of states for energy within $\pm\Delta(0)$ or $2\Delta_0$. At $T = 0$, no electrons are excited to higher states. Figure 1.12c shows effect of a finite temperature $T (< T_c)$.

The superconducting energy gap $\Delta(T)$ is now smaller than Δ_0 . A fraction of electron number is now in states above $E_F(0) + \Delta(T)$, leaving behind some unoccupied states below $E_F(0) - \Delta(T)$. The quantity $2\Delta(0)$ is the pair binding energy. It is to

**Fig. 1.13** Energy gap versus temperature**Table 1.3** Energy gap ($2\Delta_0$) (at 0°K) for some elements

Element	$2\Delta_0(\text{meV})$	$T_c(\text{K})$	$(2\Delta_0)/(k_B T_c)$
Nb	3.05	9.50	3.8
Ta	1.40	4.48	3.6
Al	0.34	1.20	3.3
Sn	1.15	3.72	3.5
Pb	2.90	7.19	4.3
Hg	1.65	4.15	4.6

Note Once set in a drift motion, a Cooper pair may be scattered only if the collision mechanism imparts an energy to the pair which is at least equal to $2\Delta_0$. But at low temperatures, this amount of energy cannot be supplied by the phonons because in superconducting state ($T < T_c$) only very low energy phonons are excited. Thus, the Cooper pair continues its drift motion indefinitely

be noted here that the energy interval 2Δ (i.e. discreteness in energy for a superconductor) is in macroscopic electron system, unlike energy gap in a semiconductor or an insulator.

The energy gap is a function of temperature and the temperature dependence is as shown in Fig. 1.13. With increasing temperature, the gap decreases and finally vanishes at $T = T_c$. In the BCS theory, it is shown that

$$\Delta(T)_{T \rightarrow T_c} = aT_c(1 - (T/T_c))^{1/2}, \quad (1.19)$$

where, in the weak coupling approximation $a = a_{\text{BCS}} = 3.06$. At temperatures below T_c , the presence of quasi-particles (normal electrons) being less than the total number of electrons.

The value of the energy gap at 0°K (i.e. $2\Delta_0$) of some of the elements is shown in Table 1.3. The ratio $2\Delta_0$ to $k_B T_c$, according to BCS theory is 3.52, which is the same for all superconductors. The ratios given in the last column of the table show good agreement with the theory. In high temperature superconductors (HTSCs), because of the layered structure, the carrier motion is quasi-two-dimensional, which favours better pairing, therefore, even carriers far from E_F bind, leading to a large value of Δ . The ratio $\Delta(0)/E_F$ indicates the fraction of carriers paired and is much larger in HTSCs than in conventional superconductors.

1.13 Thermodynamics of Superconductors

The transition to the superconducting state is a function of temperature and applied magnetic field. In pure samples, the transition is reversible and can be described by equilibrium thermodynamics. The conditions for equilibrium are found by minimising the magnetic Gibbs free energy at constant T and H .

The change from the normal to the superconducting state occurs since the Gibbs free energy in the superconducting state (G_s) is lower than its value G_N in the normal state.

$$\text{Now, } G(T, H) = U - TS + U_M, \quad (1.20)$$

where U , T , S and U_M are internal energy, temperature entropy and the magnetic energy, respectively.

For a superconductor placed in a magnetic field H_a , the magnetic energy

$$U_M = \int_0^{H_a} \mu_0 H dM = \int_0^{H_a} \mu_0 H \chi dM = -\frac{1}{2} \mu_0 \chi H_a^2 \quad (1.21)$$

(if susceptibility χ is independent of H).

Thus,

$$G(T, H_a) = U - TS - \frac{1}{2} \mu_0 \chi H_a^2, \quad (1.22)$$

$$dG = dU - d(TS) - \mu_0 d(HM) \quad (\because U_M \equiv \mu_0 HM) \quad (1.23)$$

$$\text{or } dG = dU - TdS - SdT - \mu_0 H dM - \mu_0 M dH.$$

From second law of thermodynamics,

$$\begin{aligned} dU &= TdS + \mu_0 H dM \\ \therefore dG &= -SdT - \mu_0 M dH. \end{aligned} \quad (1.24)$$

This equation can be integrated for an isothermal magnetisation

$$G(T, H_a) - G(T, 0) = - (1/2) \mu_0 \chi H_a^2$$

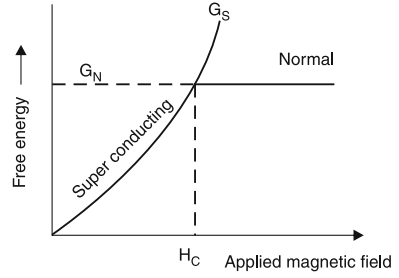
(for a metal in the superconducting state, $\chi = -1$)

$$\therefore G_s(T, H_a) - G_s(T, 0) = (1/2) \mu_0 H_a^2. \quad (1.25)$$

In the normal state, $\chi = 10^{-6}$ (emu) (i.e. for $T > T_c$) magnetisation is taken to be zero so,

$$G_N(T, H_a) = G_N(T, 0).$$

Fig. 1.14 Free energies G_S and G_N versus applied magnetic field



At $H_a = H_c$, the normal and superconducting phases are in equilibrium at the same temperature and field

$$\begin{aligned} \therefore G_s(T, H_c) &= G_N(T, H_c) = G_N(T, 0) \\ &= G_s(T, 0) + 1/2\mu_0 H_c^2(T). \end{aligned} \quad (1.26)$$

$$G_N(T, 0) - G_s(T, 0) = 1/2\mu_0 H_c^2(T).$$

For $H_a > H_c$, we have $G_s > G_N$, whereas for $H_a < H_c$, $G_s < G_N$ and therefore, the superconducting state is stable.

The above equation provides a direct measure of the condensation energy of the superconducting state, i.e. the reduction in the free energy in forming the new phases is $1/2\mu_0 H_c^2(T)$ per unit volume.

The Gibbs free energies G_S and G_N from (1.25) and (1.26) are plotted in Fig. 1.14.

Equation (1.24) can now be used to determine the entropy as

$$S = - \left(\frac{\partial G}{\partial T} \right)_H \quad (1.27)$$

using (1.26) and (1.27), we have

$$\begin{aligned} S_N &= S_s - \frac{1}{2}\mu_0 \frac{d}{dT}(H_c^2) \\ S_N &= S_s - \mu_0 \left(H_c \frac{dH_c}{dT} \right). \end{aligned} \quad (1.28)$$

Experimentally, it is observed that dH_c/dT is always negative. Therefore, entropy in the superconducting state is lower than that in the normal state, i.e. the superconducting state is more ordered than the normal state.

Further, specific heat

$$C_v^e = T \left(\frac{\partial S}{\partial T} \right) H_c. \quad (1.29)$$

Using (1.28) and (1.29), we obtain

$$\begin{aligned}
 C_N - C_S &= -\mu_0 T \frac{d}{dT} \left[H_c \frac{dH_c}{dT} \right] \\
 \text{or } C_{eN} - C_{es} &= -\mu_0 T \left[\left(\frac{dH_c}{dT} \right)^2 + H_c \frac{d^2 H_c}{dT^2} \right] \\
 \text{or } C_{es} - C_{eN} &= \mu_0 T \left[\left(\frac{dH_c}{dT} \right)^2 + H_c \frac{d^2 H_c}{dT^2} \right].
 \end{aligned} \tag{1.30}$$

Evaluated at T_c , this equation yields

$$\frac{\Delta C}{\gamma T_c} = \frac{\mu_0}{\gamma} \left(\frac{dH_c}{dT} \right)^2_{T=T_c}. \tag{1.31}$$

The electron contribution to specific heat shows two features related to opening of energy gap, when the temperature is lowered through T_c . With respect to the normal state specific heat

$$C_{eN} = \gamma T \tag{1.32}$$

$$\text{with } \gamma = 2\pi^2 k_B^2 N(0)/3. \tag{1.33}$$

C_{es} at T_c shows the jump given by

$$(C_{es} - C_{eN})/T_c = 1.43, \tag{1.34}$$

followed by an exponential decrease roughly proportional to $\exp \left[-\frac{\Delta_0}{k_B T} \right]$. The phonon specific heat does not change in the superconducting state (Fig. 1.15).

It is to be noted here that, although H_c vanishes at $T = T_c$, (dH_c/dT) does not, as a result the specific heat must exhibit a discontinuity at this temperature.

1.13.1 Latent Heat of Superconducting Transitions

Since $dQ = TdS$ for a reversible flow of heat, we find from (1.28) that the latent heat of transition from the superconducting to the normal state is

$$L = -T \mu_0 H_c \frac{dH_c}{dT}. \tag{1.35}$$

This is analogous to the Clausius–Clapeyron relation ($L = T \Delta V dP/dT$) that describes the dependence of the latent heat of a first-order transition on change of pressure with temperature and of change of volume with phase.

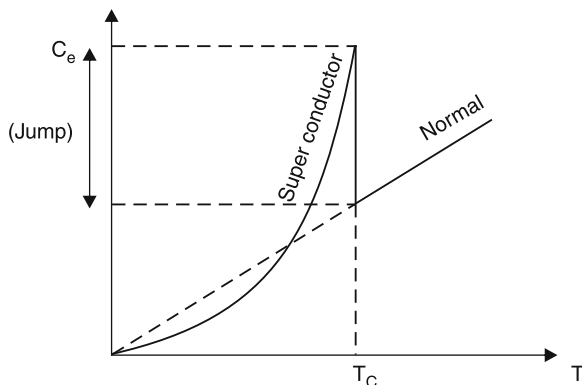
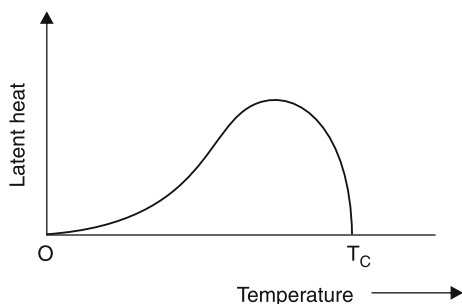


Fig. 1.15 The temperature dependence of electronic specific heat of a conductor in the normal and superconducting states

Fig. 1.16 Latent heat of a superconductor



The latent heat of transition for a superconductor is plotted in Fig. 1.16.

It seems to vanish at $T = 0$, because of Nernst theorem, and also at T_c , since H_c vanishes there.

The fact that L and $S_N - S_s$ is zero at T_c is typical of a phase transition that involves a change of order rather than a change of state. Such transitions are known as transitions of the second-order (it is to be noted that dH_c/dT is equal to zero only at $T = 0$ and $T = T_c$). Thus, although $S_s < S_N$. There is no discontinuity in S and hence, no latent heat for transition at $T = T_c$).

In contrast, for $T < T_c$, the transition to normal state induced by a field involves a finite entropy change and correspondingly, a latent heat (i.e. a change of state). This is consequently a first-order transition.

1.13.2 Heat Capacity of Superconductors

The specific heat, C_v in a normal conductor at low temperatures consists of two contributions

$$C_v = \gamma T + \alpha T^3, \quad (1.36)$$

where α and γ are constants.

For an insulator $\gamma = 0$, a pure T^3 behaviour. For metals, $\gamma \neq 0$; the linear term is a contribution from conduction electrons. The T^3 term (in both the cases) is due to lattice vibrations.

In usual superconductors, the transition has practically no effect on the lattice. From the theory of normal metals, it is known that at low temperatures $C_l^n \sim T^3$. The same dependence characterises C_l^s in the superconducting state. Whereas, the electronic contribution changes drastically and is given by an exponential decay (of C_{el}^s) as $T \rightarrow 0$. This behaviour is explained as follows:

Because of the energy gap, the number of quasi-particles (excited across the gap) varies roughly by a Boltzmann factor $\exp(-\Delta/k_B T)$.

At finite temperature, the quasi-particles behave just like ordinary electrons and are given by

$$n = \left[\exp\left(\frac{\epsilon}{T}\right) + 1 \right]^{-1}, \quad (1.37)$$

$$\text{where } \epsilon = \sqrt{\epsilon'^2 + \Delta^2(T)} \quad (1.38)$$

$$\text{and } \Delta(T) \big|_{T \rightarrow T_c} = a' T_c \left(1 - \frac{T}{T_c}\right)^{\frac{1}{2}}. \quad (1.39)$$

ϵ' is the normal metal electron energy given by

$$\epsilon' = \left(\frac{p^2}{2m^*} - E_F \right) \quad (1.40)$$

and in weak coupling approximation $a' = 3.06$ (BCS limit).

Because of the appearance of $\Delta(T)$ term in ϵ , the number of excitations n of a given energy is less than the corresponding number of electrons in a normal metal (at $T < T_c$). (It is to be noted here that for $T \geq T_c$, $\Delta = 0$, the excitations vanish and the function given by (1.37) becomes the usual expression for electrons in a normal metal). Thus, superconductor is described by a two fluid model, which has normal electrons and a “superconducting” component.

For $T \ll T_c$, the heat capacity is given by

$$\frac{C_{el}^s(T)}{C_{el}^n(T_c)} = \left[\frac{3\sqrt{2}}{\pi} \frac{\Delta(0)}{T_c} \right] \left(\frac{\Delta(0)}{T} \right)^{3/2} e^{-\frac{\Delta(0)}{T}}. \quad (1.41)$$

Therefore, presence of energy gap leads to electronic heat capacity behaving radically different from normal metal result ($C_{\text{el}}^{\text{n}} \sim T$).

In weak coupling (i.e. BCS) case

$$\frac{\Delta(0)}{T_c} = 1.76. \quad (1.42)$$

At $T = T_c$, there is a jump in the heat capacity. When the temperature is reduced, the specific heat jumps to a higher value at $T = T_c$ and then falls much more rapidly as $e^{-\Delta(0)/T}$ for $T < T_c$.

$$\frac{C_{\text{el}}^{\text{s}}}{\alpha T_c} = a \exp\left(-\frac{b T_c}{T}\right), \quad (1.43)$$

where αT_c is the “low temperature” electronic specific heat of normal state, a and b are constants, independent of temperature ($a \approx 9$, $b \approx 1.5$). The size of the discontinuity in specific heat at $T = T_c$ is 2.5 in units of αT_c .

1.13.3 Strong Coupling Case

In BCS theory

$$2\Delta = 3.52 T_c, \quad (1.44)$$

$$\frac{C_{\text{s}} - C_{\text{n}}}{C_{\text{n}}} = 1.43. \quad (1.45)$$

These formulae are of a universal character.

The universality is due to the fact that the BCS theory was developed in the weak coupling approximation, i.e. electron–phonon interaction was assumed to be weak (and coupling constant $\lambda < 1$). However, there were some pronounced deviations from this universality, e.g. for Pb–Bi alloy, $2\Delta = 5T_c$. The experimentally observed deviations are caused by the fact that electron–phonon coupling is not weak. Thus, the effect of strong coupling must be taken into account. The foundation of the theory of strong coupling is formed by an equation derived by Eliashberg in 1960. This equation contains a very important term

$$g(\Omega) = \alpha^2(\Omega) F(\Omega),$$

where $F(\Omega)$ equals density of states of lattice vibrations and $\alpha^2(\Omega)$ describes interaction between electrons and the lattice. Thus, it describes both the state of the phonon system and the electron–phonon interaction.

Geilikman and Kresin in 1966 obtained the following formula for the energy gap

$$\frac{2\Delta(0)}{T_c} = 3.52 \left[1 + \alpha \left(\frac{T_c}{\bar{\Omega}} \right)^2 \ln \left(\frac{\bar{\Omega}}{T_c} \right) \right], \quad (1.46)$$

where $\alpha = 5.3$ and $\bar{\Omega}$ is the characteristic frequency of lattice vibrations. The second term in brackets is the correction due to strong coupling. The temperature dependence of energy gap changes from

$$\begin{aligned} \frac{\Delta(T)}{T_c} &= a \left[1 - \left(\frac{T}{T_c} \right) \right]^{\frac{1}{2}}, \quad (a_{\text{BCS}} = 3.06), \\ \frac{\Delta(T)}{T_c} &= 3.06 \left[1 + 8.8 \frac{T_c^2}{\bar{\Omega}^2} \ln \left(\frac{\bar{\Omega}}{T_c} \right) \right]. \end{aligned} \quad (1.47)$$

(Note: factor 2 is inclusive in $\Delta(T)$).

1.14 London Equations and Penetration Depth

The two basic electrodynamics properties, viz. perfect conductivity and perfect diamagnetism, were well described in 1935 by F. London and H. London, who proposed two equations (known as London equations) to govern the microscopic electric and magnetic fields.

It was shown by London brothers that the magnetic flux lines are not completely expelled from a superconductor rather they remain confined in a thin surface layer called the *penetration depth*. They postulated a two fluid model for electrons with super-fluid and normal densities n_s and n_n (and velocities v_s and v_n , respectively). If n_o denotes number of electrons per unit volume, then

$$n_0 = n_s + n_n. \quad (1.48)$$

The equation of motion for super fluid electrons is

$$m \frac{d\vec{v}_s}{dt} = -e \vec{E}. \quad (1.49)$$

The current density of the super fluid electrons is

$$\vec{J}_s = -en_s v_s. \quad (1.50)$$

Equation (1.49) and (1.50) yield

$$\frac{d\vec{j}_s}{dt} = \frac{n_s e^2}{m} \vec{E}. \quad (1.51)$$

This is called the *first London equation*. Taking curl of this equation,

$$\begin{aligned} \nabla \times \frac{d\vec{j}_s}{dt} &= \left(\frac{n_s e^2}{m} \right) \text{curl } \vec{E} \\ \text{or } \nabla \times \frac{d\vec{j}_s}{dt} &= -\frac{n_s e^2}{m} \left(\frac{\partial \vec{B}}{\partial t} \right) \end{aligned}$$

using Maxwell's equation.

Integrating the above expression with respect to time and choosing the constant of integration to be zero (for consistency with Meissner effect), we have

$$\nabla \times \vec{j}_s = -\left(\frac{n_s e^2}{m} \right) \vec{B}. \quad (1.52)$$

This is called the *second London equation*. We may derive the Meissner effect from the second London equation by using Maxwell's equation

$$\nabla \times \vec{B} = \mu_0 \vec{j}_s. \quad (1.53)$$

Taking the curl of this equation

$$\nabla(\nabla \cdot \vec{B}) - \nabla^2 \vec{B} = \mu_0 \nabla \times \vec{j}_s. \quad (1.54)$$

Since $\nabla \cdot \vec{B} = 0$, therefore

$$\nabla^2 \vec{B} = \frac{1}{\lambda^2} \vec{B} \quad (\text{using (1.52)}), \quad (1.55)$$

$$\text{where } \lambda = \left(\frac{m}{\mu_0 n_s e^2} \right)^{\frac{1}{2}} \text{ is called London penetration depth.} \quad (1.56)$$

The solution of the (1.55) for $\vec{B} = \vec{B}(x)$ is of the form

$$\vec{B}(x) = B_0 e^{-\frac{x}{\lambda}} \quad (\text{see Fig. 1.17}) \quad (1.57)$$

Thus, \vec{B} does not penetrate very deeply into a superconductor, rather penetrates only a distance λ within the surface (it implies the *Meissner effect*)

From (1.51) and (1.52) we have two equations

Fig. 1.17 Decay of the magnetic field penetrating in a superconducting half space (existing for $x \geq 0$)

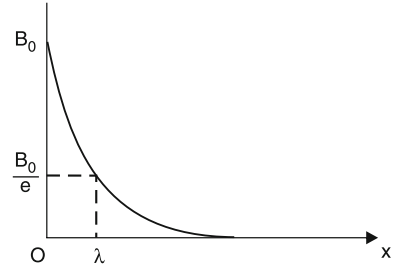
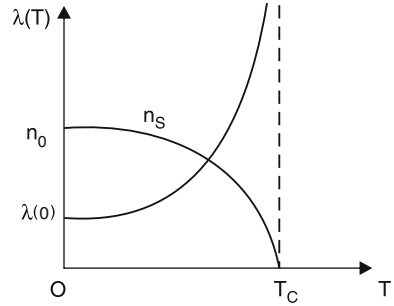


Fig. 1.18 Variation of penetration depth and n_s with temperature



$$\vec{E} = \frac{\partial}{\partial t} (\wedge \vec{j}_s) \quad (1.58)$$

$$\text{and } \vec{B} = -\text{curl} (\wedge \vec{j}_s), \quad (1.59)$$

which govern the microscopic electric and magnetic fields, where

$$\wedge \equiv \left(\frac{m}{n_s e^2} \right) \quad (1.60)$$

is a phenomenological parameter. The number density of electrons depends on temperature and varies from zero at T_c to a limiting value of the order n_0 , the density of conduction electron at $T \rightarrow 0^\circ \text{K}$ (Fig. 1.18).

The penetration depth λ also depends on temperature as

$$\lambda(T) = \lambda(0) \left[1 - \left(\frac{T}{T_c} \right)^4 \right]^{-\frac{1}{2}}. \quad (1.61)$$

The density of super electrons n_s also varies with temperature as

$$n_s = n_0 \left[1 - \left(\frac{T}{T_c} \right)^4 \right], \quad (1.62)$$

where $n_0 = n(0)$

$$(\equiv n(T)_{T=0K}).$$

1.15 Ginzberg–Landau Theory

There are basically two theoretical approaches to describe various superconducting phenomena (1) a phenomenological theory effective through the London equations and (2) the microscopic (BCS) theory.

However, the comprehensive theoretical picture remain incomplete without considering the impact and consequences of yet another theory known as the Ginzberg–Landau (GL) theory proposed 7 years prior to the BCS theory.

According to Landau, an ordered thermodynamic phase is characterised by a non-zero order parameter, accordingly Ginzberg and Landau introduced a complex pseudo-wave function ψ as an order parameter within Landau's general theory of second-order phase transitions. This ψ vanishes at $T \geq T_c$. The GL theory has accorded a semi-phenomenological status. Near the critical temperature $|T - T_c| \leq T_c$, the theory is very much simplified and the behaviour is described by GL equations.

According to London, the wave function of the superconducting electrons is rigid, i.e. it does not change when a magnetic field is applied. In GL theory, the absolute rigidity is modified and parameter ψ is defined, such that

$$|\psi|^2 = n_s, \quad (1.63)$$

the density of super-electrons.

More physically, ψ can be thought of as the wave function of the center of mass motion of the Cooper pairs (In fact, it was shown by Gorkov in 1959, that the GL theory was a limiting form of the microscopic theory of BCS, valid near T_c in which ψ is directly proportional to the gap-parameter Δ).

Since the phenomenon of superconductivity is a second-order phase transition, there is a critical temperature T_c and a positive parameter n_s , which is zero when $T > T_c$ and is finite when $T < T_c$.

The Gibbs free energy F can be expanded as

$$F(T, V, n_s) = F(T, V, 0) + \alpha n_s + (1/2)\beta n_s^2. \quad (1.64)$$

The equilibrium condition $\partial F / \partial n_s = 0$ gives

$$\alpha + \beta n_s = 0 \quad \text{or} \quad n_s = -\frac{\alpha}{\beta}, \quad (1.65)$$

Since F is to be minimum, therefore

$$\frac{\partial^2 F}{\partial n_s^2} > 0.$$

So β is positive (from (1.64)) and α should be negative (from (1.65)). To obtain a phase transition of second kind, we assume

$$\begin{aligned} \alpha(T_c) &= 0; \quad \beta(T_c) > 0, \\ \alpha(T) &= (T - T_c) \left(\frac{\partial \alpha}{\partial T} \right)_{T=T_c}. \end{aligned} \quad (1.66)$$

(for $T < T_c$, $\alpha(T) < 0$ and $\beta(T) > 0$).

Substituting for n_s from (1.65) into (1.64), we have

$$F_s = F_n - \frac{\alpha^2}{2\beta}. \quad (1.67)$$

$$\text{But } (F_s - F_n) = -\frac{H_c^2}{8\pi}.$$

so, we have

$$\frac{\alpha^2}{2\beta} = \frac{H_c^2}{8\pi}. \quad (1.68)$$

Here, n_s is always constant and the magnetic field enters as a term $\frac{H_c^2}{8\pi}$ in the free energy of the superconducting phase.

Since ψ is a kind of effective wave function, in presence of an external magnetic field H , the free energy will not only increase by $\frac{H^2}{8\pi}$ per unit volume, but also by an extra term connected by the gradient of ψ (because ψ is not rigid in the presence of the magnetic field). To preserve the gauge invariance, GL assumed the extra term to be

$$\frac{1}{2m} \left| -i\hbar \nabla \psi + \frac{e^*}{c} \vec{A}(\vec{r}) \psi \right|^2,$$

where $\vec{A}(\vec{r})$ is the vector potential of the applied field H , and e^* the effective charge. Thus,

$$F_s = F_n + \int \left\{ \alpha |\psi|^2 + \frac{1}{2} \beta |\psi|^4 + \frac{H_c^2}{8\pi} + \frac{1}{2m} \left| -i\hbar \nabla \psi - \frac{e^*}{c} \vec{A}(\vec{r}) \psi \right|^2 \right\} dv. \quad (1.69)$$

This expression is gauge-invariant under the simultaneous transformation

$$\begin{aligned}\psi' &= \psi \exp \left(\frac{ie^*}{\hbar c} \right) \phi. \\ \vec{A}' &= \vec{A} + \nabla \phi, \\ [\text{In fact } e^* &= 2e].\end{aligned}\tag{1.70}$$

We now minimise the expression with respect to ψ^* and \vec{A} . Variation with respect to ψ^* gives

$$\delta F = \int \left\{ \alpha \psi + \beta |\psi|^2 \psi + \frac{1}{2m} \left[\left(-i\hbar \nabla \psi - \frac{e^* \psi}{c} \right) \left(i\hbar \nabla - \frac{e^*}{c} \vec{A} \right) \right] \right\} \delta \psi^* dv. \tag{1.71}$$

Integrating the last term by parts gives

$$\frac{1}{2m} \left(\int \delta \psi^* \left(-i\hbar \nabla - \frac{e^*}{c} \vec{A} \right)^2 \psi dv + \iint \hat{n} \cdot \left(-i\hbar \nabla - \frac{e^*}{c} \vec{A} \right) \psi \delta \psi^* da \right). \tag{1.72}$$

The surface integral vanishes because $\delta \psi^*$ is arbitrary and, therefore, the boundary condition is

$$\hat{n} \cdot \left(-i\hbar \nabla - \frac{e^*}{c} \vec{A} \right) = 0. \tag{1.73}$$

Hence, we get from (1.71)

$$\frac{1}{2m} \left(-i\hbar \nabla - \frac{e^*}{c} \vec{A} \right)^2 \psi + \alpha \psi + \beta |\psi|^2 \psi = 0. \tag{1.74}$$

Note that this is analogous to the Schrödinger equation for a free particle, but with a nonlinear term. This equation describes the equilibrium spatial variation of ψ . Variation with respect to \vec{A} yields,

$$\nabla \times \nabla \times \vec{A} = -\nabla^2 \vec{A} = \frac{4\pi}{c} \vec{J} \tag{1.75}$$

(using the gauge $\nabla \cdot \vec{A} = 0$), where

$$\vec{J} = -\frac{ie^*\hbar}{2m} (\psi^* \nabla \psi - \psi \nabla \psi^*) - \frac{e^{*2}}{mc} |\psi|^2 \vec{A} \tag{1.76}$$

is the same as the usual quantum mechanical current expression for particles of charge e^* and mass m .

So the fundamental equations of the GL theory are

$$\frac{1}{2m} \left[-i\hbar \nabla - \frac{e^*}{c} \vec{A} \right]^2 \psi + \alpha \psi + \beta |\psi|^2 \psi = 0 \quad (1.77)$$

and

$$\vec{J} = \frac{e^* \hbar}{2im} (\psi^* \nabla \psi - \psi \nabla \psi^*) - \frac{e^{*2}}{mc} |\psi|^2 \vec{A}. \quad (1.78)$$

With this formalism, Ginzberg and Landau were able to treat two features, which were beyond the scope of the London theory, namely

- (1) Nonlinear effects of fields strong enough to change n_s (or $|\psi|^2$) and
- (2) The spatial variation of n_s

This will be discussed in the subsequent section, while considering the variation of $|\psi|^2$ in type-I and type-II superconductors. Thus, GL theory embodies in a simple way the macroscopic quantum mechanical nature of the superconducting state.

1.16 Type-I and Type-II Superconductors

Both coherence length and penetration depth diverge in the same way near $T = T_c$. So, a constant k is defined

$$\text{as } k = \frac{\lambda}{\xi}, \quad (1.79)$$

which will remain finite as $T \rightarrow T_c$.

This is known as *Ginzberg–Landau parameter* and can be considered as a characteristic of a material. The magnitude of k defines two kinds of superconductors. For $k \ll 1$ (i.e. $\lambda \ll \xi$), we have type-I superconductors and superconductors having $k \gg 1$ (i.e. $\lambda \gg \xi$) are type II superconductors. Figure 1.19a, b depicts spatial dependence of the order parameter $\psi(x)$ and the magnetic field $H(x)$ at the superconductor-normal interface, for respectively type-I and type-II superconductors.

Consider a plane boundary between the superconducting (S) and normal (N) regions in the same material. At the boundary, the magnetic flux density must rise from zero in the superconductor to H_c in the normal region, over a distance \sim penetration depth λ (as required by the condition for thermodynamic equilibrium). Likewise, the superconducting wave function ψ , and hence the density of paired electrons must fall to zero over a distance $\sim \xi$ (the coherence length). Thus, the formation of a S–N boundary involves an increase in energy (or loss of condensation energy $\approx \xi_0 \left(\frac{\mu_0 H_c^2}{2} \right)$ per unit area and a reduction in the magnetic energy $\approx \lambda_0 \left(\frac{\mu_0 H_c^2}{2} \right)$ per unit area).

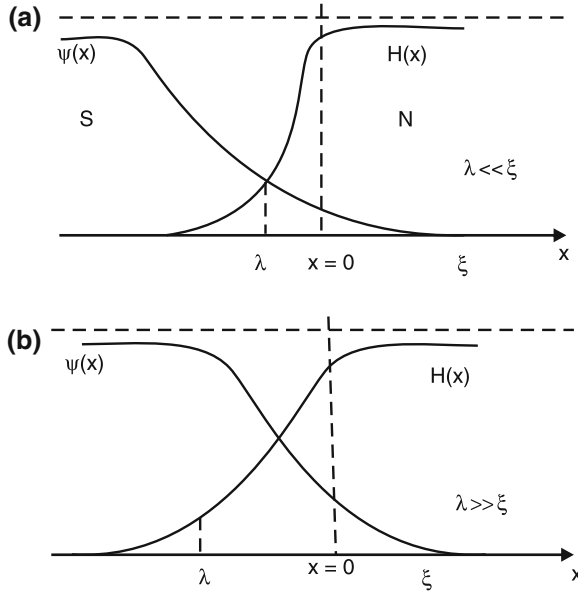


Fig. 1.19 **a** type-I and **b** type-II superconductors

The sign of the surface energy

$$\sigma_s = (\xi - \lambda) \frac{\mu_0 H_c^2}{2} \quad (1.80)$$

is then determined by the relative magnitudes of the coherence and penetration lengths. Thus, a type-I superconductor has a positive surface energy and type-II superconductor has a negative surface energy in an applied magnetic field. Type-I superconductors show complete Meissner effect. The magnetisation versus applied magnetic field is shown in Fig. 1.20. The magnetisation drops suddenly at the critical field $H = H_c$ (Fig. 1.21).

In type-II superconductor, magnetisation drops earlier, before reaching the critical field $H = H_c$. There starts penetration of flux in the specimen at a field value H_{c1} (which is lower than H_c). The electrical properties in the superconducting state are also seen upto a field H_{c2} (which is greater than H_c). H_{c1} and H_{c2} are known as the lower and upper critical fields respectively.

The state between H_{c1} and H_{c2} is known as the mixed state or *vortex state* (because there is partial flux penetration and there are both superconducting and normal regions in the form of vortices). At $H \geq H_{c2}$, the superconductivity is destroyed. The phase change at H_c represents a first-order transition. The transitions at H_{c1} and H_{c2} are of second-order.

$$\text{The free energy } F_n > F_s. \quad (1.81)$$

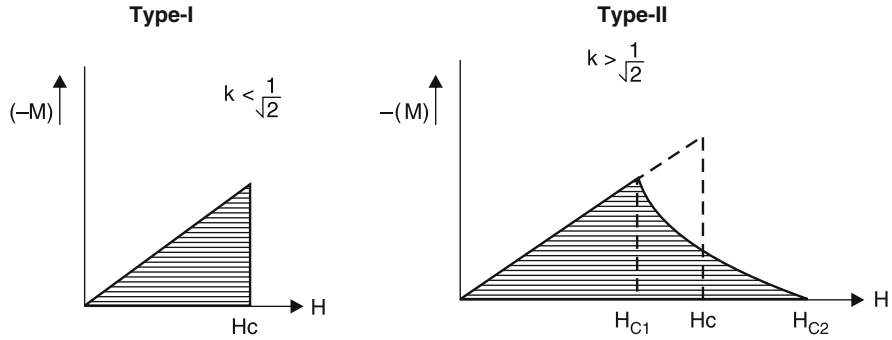


Fig. 1.20 Magnetisation versus applied magnetic field for type-I and type-II superconductors

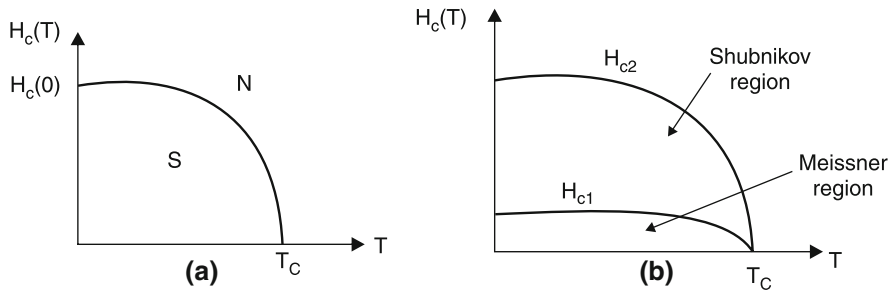


Fig. 1.21 Critical magnetic field as a function of temperature for **a** type-I and **b** type-II superconductors

The free energy cost per unit surface area ($F_n - F_s$) results from sacrificing the condensation energy in a layer of width ξ (the coherence length), i.e.

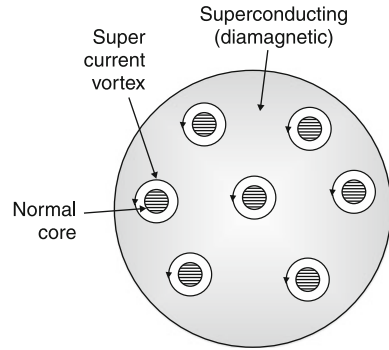
$$\Delta F_{\text{cost}} \text{ varies as } \left(\frac{H_c^2}{2\mu_0} \right) \xi, \quad (1.82)$$

where H_c is known as the thermodynamic critical field. The free energy of a superconductor increases in an applied field. The free energy-gain derives from allowing the field to invade a distance equal to the penetration depth λ , i.e.

$$\Delta F_{\text{gain}} \sim - \left(\frac{H_{\text{app}}^2}{2\mu_0} \right) \lambda. \quad (1.83)$$

Clearly ΔF_{gain} dominates for $\lambda > \xi$ as in a type-II superconductor. When H exceeds H_{c1} , the free energy is lowered by maximising the S/N interface area ($H > H_{c1} \Rightarrow B \neq 0$).

Fig. 1.22 The *triangular* lattice of vortices in the mixed state



Flux enters at $H > H_{c1}$ and according to Abrikosov, it does so in the form of flux vortices, which assume a triangular lattice structure to minimise their interaction energy. For $H_{c1} < H < H_{c2}$, we have this intermediate phase or Shubnikov phase.

At H_{c1} , the first vortex is nucleated and with increasing field, their equilibrium separation is reduced, such that at H_{c2} the normal cores overlap and then, bulk of the material turns normal (Fig. 1.22).

A vortex consists of a normal core (a cylinder of normal region parallel to the applied magnetic field) carrying a flux quantum $\phi_0 = 2.07 \times 10^{-15}$ Webers and diameter 2ξ . This microscopic normal region is surrounded by circulating super-electrons. At the centre of the core, the field is maximum and it drops to $1/e$ of its maximum value over a distance λ . A flux vortex is also known as a *fluxoid* (Fig. 1.23).

In the space between the vortices, the material remains superconducting; this is where the electric current flows, so the electrical resistance is still absent.

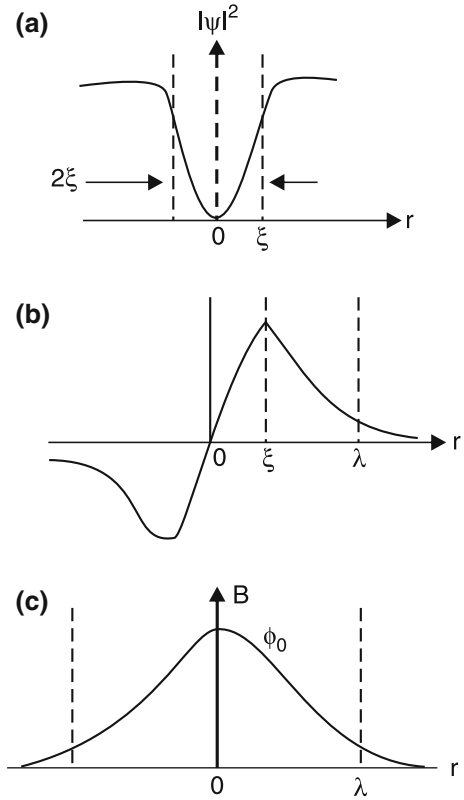
1.16.1 How a Normal Core is Formed in Mixed State?

With the application of the field $H > H_{c1}$, normal cores are nucleated, each carrying a quantum of flux ϕ_0 . A core is surrounded by a circulating current (of super-electrons), whose super-fluid velocity is quantised to the value

$$v_{s0} = \frac{\hbar}{2m\xi}. \quad (1.84)$$

The super-electrons revolve around the vortex-axis like current in a superconducting ring. The closer the superelectron to the vortex-axis, the faster it circulates. At a shorter distance from the axis, the speed exceeds the critical value v_{s0} and superconductivity is destroyed (inside normal core).

Fig. 1.23 Structure of a vortex line **a** order parameter
b current density **c** local field



1.16.1.1 The Upper Critical Field

If the number density of vortex lines is n in a specimen, then spacing “ a ” between the neighbouring lines is given by

$$a = \left(\frac{n}{3}\right)^{\frac{1}{4}} \left(\frac{\phi_0}{B}\right)^{\frac{1}{2}}. \quad (1.85)$$

With increasing field, the density of flux lines approaches the value such that $Ba^2 \sim \phi_0$. Clearly, when “ a ” reaches the value ξ , the whole sample is comprised of touching normal cores, so that we may identify the upper critical field H_{c2} with this limit and

$$H_{c2} = \frac{\phi_0}{2\pi\xi^2}. \quad (1.86)$$

It is to be mentioned here that around the surface of a normal core, there are screening currents flowing in the surface in the opposite sense to the circulating persistent currents, as a result, the diamagnetism of the bulk is maintained.

From Fig. 1.23, it is seen that $|\psi|^2$ is reduced to a small value over a length ξ and the magnetic field of a flux line is spread over a region of size λ . Thus, there is a gain of energy by letting the magnetic field in over an area λ^2 and a loss of energy, because it is not superconducting effectively over an area ξ^2 . Therefore, flux penetration is energetically favoured, if $\lambda > \xi$ (Type-II superconductor). However, if $\lambda < \xi$, fluxoids are not energetically favoured (for type-I superconductor). The lower critical field H_{c1} is defined as the value of the applied field at which it is energetically favourable to form an isolated fluxoid.

$$H_{c1} = \frac{H_c}{k\sqrt{2}} \quad \text{where } k \text{ is GL parameter.} \quad (1.87)$$

For the formation of an isolated fluxoid, the necessary condition is $\lambda > \xi$. A detailed treatment modifies this to

$$k > \frac{1}{\sqrt{2}}. \quad (1.88)$$

The value of k increases with normal state resistance ρ and in the dirty-limit (i.e. when $\ell < \xi_0$ where ℓ is mean free path)

$$k = k_0 + 2.4 \times 10^6 \rho \gamma^{\frac{1}{2}}, \quad (1.89)$$

where k_0 is the pure material value and γ is Sommerfeld constant. That is, many alloys and compounds have $\lambda > \xi$ and exhibit type-II superconductivity, but since both λ and ξ are affected by the electron mean free path (ℓ), type-I material (elements) can be made type-II by appropriate alloying (to reduce ℓ).

1.17 Why Materials with High T_c Tend to Fall in Type-II Category?

The reason qualitatively is as follows. The coherence length represents extension of the order parameter (the wave function of the super electrons). Using the position momentum uncertainty relation, we write

$$\xi = \frac{\hbar}{\Delta p}, \quad (1.90)$$

where Δp is the uncertainty in momentum. But a super-electron lies within an energy interval $k_B T_c$ from the Fermi surface and hence, the uncertainty of its energy is

$$\Delta E \cong k_B T_c. \quad (1.91)$$

Since $E = p^2/(2m)$, it follows that

$$\Delta E = p \frac{\Delta p}{m} \quad (1.92)$$

or $\Delta p \sim \Delta E = k_B T_c$ which, when substituted into (1.1) gives

$$\xi \propto \frac{1}{T_c}. \quad (1.93)$$

Therefore, the greater the T_c , the shorter the coherence length.

Transition metals and alloys usually fall in the type-II category. Their coherence length is shortened by the relatively large amount of scattering present.

Nearly 25 years ago, all known superconductors were having $T_c < 20$ K.

1.18 Why It is Extremely Difficult to Obtain Higher T_c ?

From the microscopic (BCS) theory, the T_c is given by

$$k_B T_c = (\hbar\omega) e^{-1/\lambda_{\text{eff}}}, \quad (1.94)$$

$$\text{or } k_B T_c \cong (k_B \theta) e^{-1/\lambda_{\text{eff}}}, \quad (1.95)$$

$k_B \theta$ denotes the energy-range near the Fermi level, in which conduction electrons attract to form Cooper pairs.

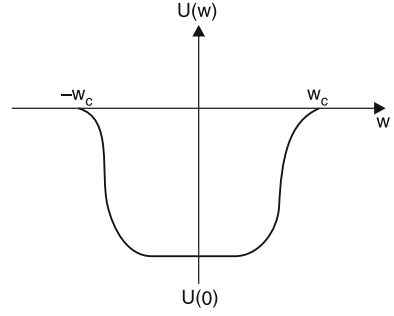
- (1) If “attraction” is due to interaction with phonons, then $\theta = \theta_D$, the Debye temperature of the material.
- (2) $k_B \theta_D$ is of the order of $\hbar\omega_D$, i.e. energy of highest frequency of phonons that can propagate in the substance.
- (3) λ_{eff} characterises the attractive force within the framework of the BCS theory (i.e. in the weak coupling limit).

$$\lambda_{\text{eff}} = N(0)V \ll 1, \quad (1.96)$$

where $N(0)$ is density of states in normal phase at the Fermi level, V is average matrix element of the interaction energy U between the electrons. λ_{eff} is a measure of the attractive force (Fig. 1.24).

The BCS model (the weak coupling case) gives

Fig. 1.24 Interaction energy between the electrons



$$\frac{2\Delta(0)}{k_B T_c} = 3.53 \quad (1.97)$$

$$\text{and } \Delta C = 1.43 T_c, \quad (1.98)$$

where ΔC is specific heat jump at T_c and γ is coefficient in the law

$$C_n = \gamma T$$

for electronic specific heat in normal state.

If the coupling is weak, then, within the phonon-mechanism

$$T_c \ll \theta_D. \quad (1.99)$$

Specifically for $\lambda_{\text{eff}} = 1/2$ and $\theta = \theta_D$, the T_c is $0.135 \theta_D$, i.e.

$$T_c < 40 \text{ K for } \theta_D < 300 \text{ K}. \quad (1.100a)$$

With an increase in λ_{eff} , phonon frequencies become lower, θ_D falls

$$\therefore T_c \sim 20 - 40 \text{ K}. \quad (1.100b)$$

References

1. Steglich et al., Phys. Rev. Lett. **43**, 1892 (1979)
2. Jerome et al., J. Phys. Lett. **41L**, 195 (1980)
3. J.G. Bednorz, K.A. Muller, Z. Phys. **B64**, 189 (1986)
4. M.K. Wn, C.W. Chu, Phys. Rev. Lett. **58**, 908 (1987)
5. H. Maeda et al., Jpn. J. Appl. Phys. **27**, L209 (1988)
6. Z.Z. Sheng, A.M. Hermann, Nature **332**, 55 (1988)
7. Hebard et al., Nature **350**, 600 (1991)



<http://www.springer.com/978-3-642-28480-9>

High-Temperature Superconductors

Saxena, A.K.

2012, XVIII, 258 p., Hardcover

ISBN: 978-3-642-28480-9